Supporting information

Supporting Table 1: Crystallographic contacts of the dynamic loop of wild-type hNgb.

First residue	Second residue	Distance (Å)
GlnA48 O	CysA120# NE2	3.2
PheA49 O	ArgB30# NH1	2.94
SerA50 OG	TyrB115# OH	2.66
GluA53 O	LysB119# NZ	2.81
GluA60 OE1	TyrB115# OH	2.62
ArgB47 NH1	CysB120# O	2.82
GlnB48 OE1	SerB104# N	3.05
GlnB48 OE1	SerB104# OG	2.74
SerB51 OG	ArgB97# NH2	2.81
AspB54 OD1	ArgB97# NH1	2.80
AspB54 OD2	TrpB148 NE1	3.17

Supporting Table 2: Close contacts within 4 Å and hydrogen bonds between the heme and wild-type hNgb.

Porphyrin atom (molecule)	hNgb atom	Distance Å
CMB (A)	LeuA38 CD2	4.0
CMB (A)	PheA42 CZ	3.4
C2B (A)	PheA42 CZ	3.5
Fe (A)	HisA64 NE2	2.0
O1A (A)	Lys67 NZ	4.2
C4C (A)	ValA68 CG2	3.6
CBC (A)	ValA71 CG1	3.5
CAC (A)	ValA71 CB	3.7
CMD (A)	LeuA92 CD1	3.6
C2D (A)	LeuA92 CD1	3.5
C1D (A)	LeuA92 CD1	3.9
CHD (A)	LeuA92 CD1	3.9
Fe (A)	PheA96 NE2	2.1
CHB (A)	ValA101 CG2	3.6
CMB (A)	ValA101 CG1	3.7
CBB (A)	PheA106 CE1	3.8
CMC (A)	PheA106 CE1	3.7
CHC (A)	PheA106 CE	3.5
CBB (A)	ValA109 CG2	3.5
CAB (A)	ValA109 CG2	3.7
CMB (A)	LeuA38 CD2	4.0
CHB (B)	PheB42 CE1	3.6
CMC (B)	PheB42 CZ	3.6
Fe (B)	HisB64 NE2	2.1
O1A (B)	LysB67 NZ	2.7
CBC (B)	ValB68 CG1	3.9
C3C (B)	ValB68 CG2	3.6
CBC (B)	ValB71 CG1	3.7
CAC (B)	ValB71 CB	3.7
CMD (B)	LeuB92 CD1	3.5
C2D (B)	LeuB92 CD1	3.4
CMD (B)	LeuB92 CD1	3.5
Fe (B)	PheB96 NE2	2.1
CMB (B)	ValB101 CG2	3.8
CBB (B)	ValB101 CG1	4.0
CAC (B)	PheB106 CE1	3.8
CMC (B)	PheB106 CE1	3.8
CMC (B)	ValB109 CG1	3.6
CAB (B)	ValA109 CG2	3.6

Supporting Figures

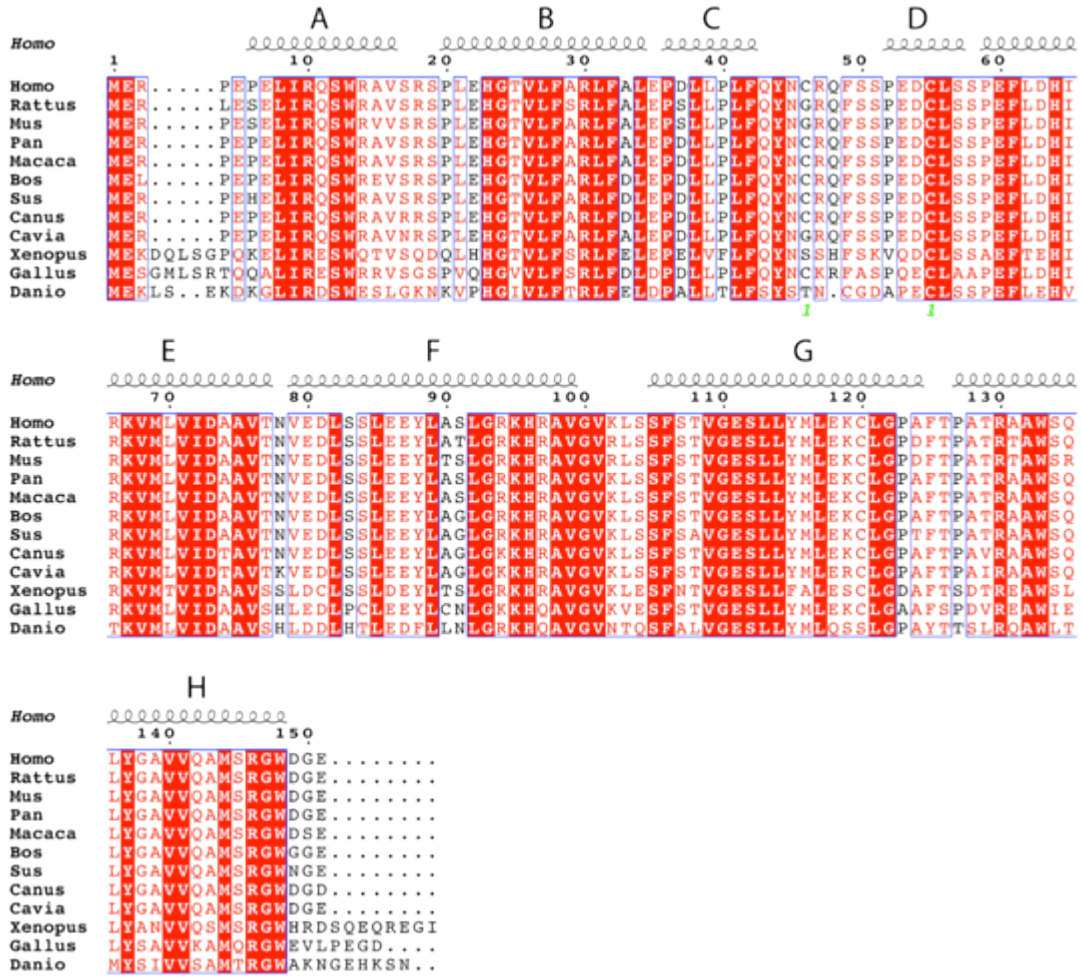

Supporting Figure S1: Sequence alignment of Ngbs.
Multiple sequence alignment of various Ngbs (*Homo sapiens*, *Rattus norvegicus*, *Mus musculus*, *Pan troglodytes*, *Macaca mulatta*, *Bos Taurus*, *Sus scrofa*, *Canus lupus familiaris*, *Cavia porcellus*, *Xenopus tropicalis*, *Gallus gallus*, *Danio rerio*) calculated with *ClustalW*. This figure was drawn with *ESPript*. The secondary structural elements of monomer B of wild-type hNgb are shown above. The position of the cysteine residues forming the intramolecular disulfide bond is indicated in green.

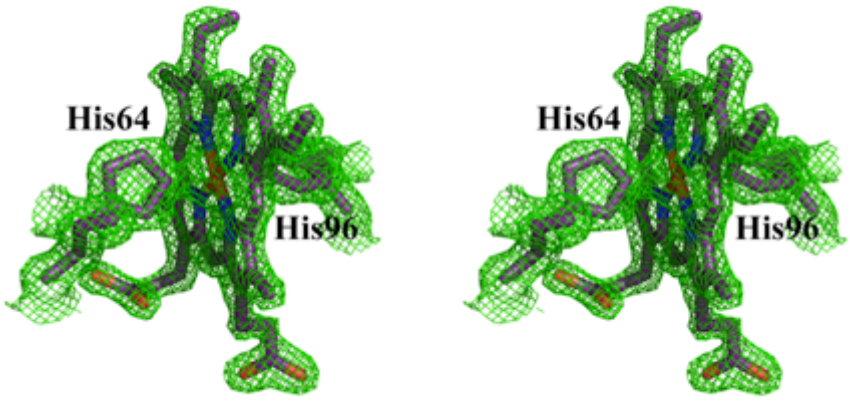

Suporting Figure S2: Stereoview of the heme and the two histidine ligands of molecule A of wild-type hNgb with Fobs-Fcal omit map contoured at 1.5 σ.

Only one heme orientation (with the side chain of Phe42 contacting the methyl groups at the 1 and 8 heme positions) is observed in both monomers of wild-type hNgb, as indicated by the electron density. This absence of heme conformational disorder is attributed to the close contacts that are formed between the porphyrin and the protein on the heme side opposite to the propionate groups (Table S3). The average B-factors of the His64 side chain of 11.6 $Å^2$ for both molecules (compared to 16.7 $Å^2$ for His96), are in the average B-factors for the whole molecule, which does not point to an increased mobility of His64. The conformation of the His64 side chain is locked by a H-bond with a water molecule that bridges the Nδ1 atom and the carboxy oxygen atom of Phe61. In contrast, indication of heme of heterogeneity both in mouse and human Ngbs, with the presence of two alternative heme orientations within the heme pocket, was provided by X-ray crystallography and NMR. It was proposed that the lack of orientational selectivity is related to the presence of the very large cavity lining the heme, a cavity that is much smaller in wild-type hNgb.

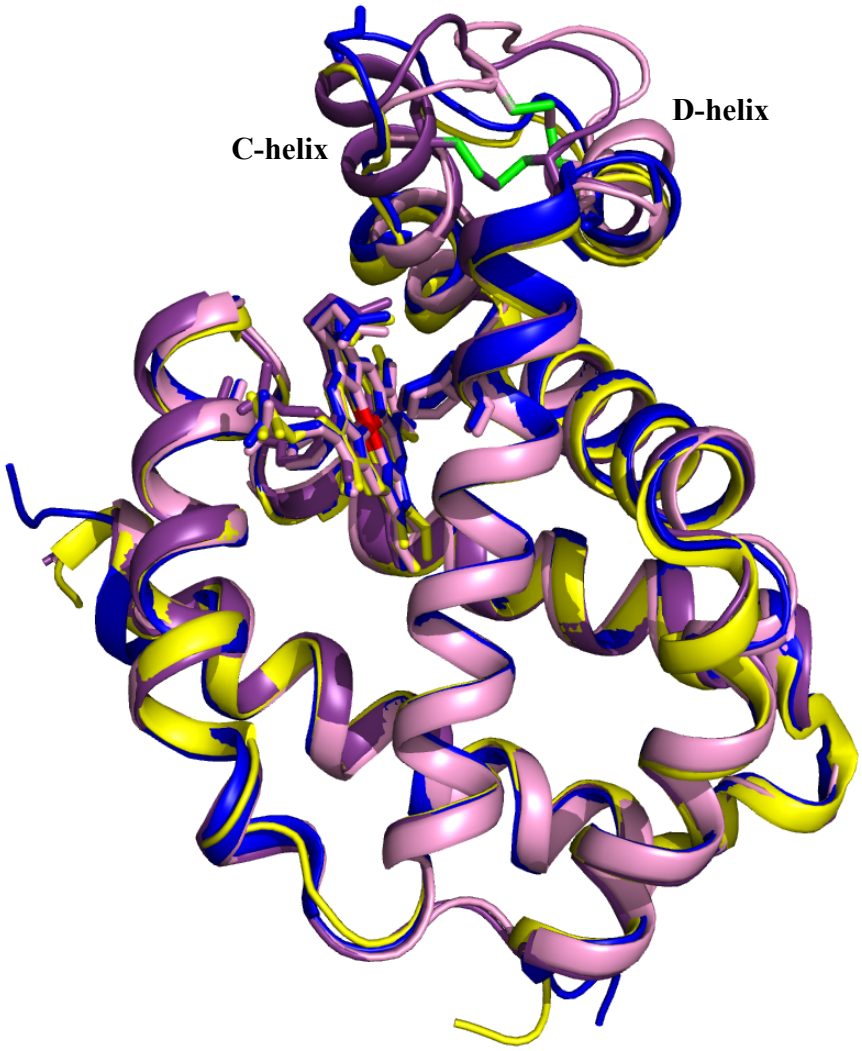

Supporting Figure S3: Superposition of mouse Ngb, wild-type and mutant hNgbs. Regions 3-35 and 60-149 of wild-type hNgb (molecule A colored in violet and molecule B colored in pink) and mouse Ngb (PDB code 1Q1F colored in yellow) were superimposed with molecule B of mutant hNgb (PDB code 1OJ6 colored in dark blue). The conformations of the heme and the imidazole side-chain of the distal histidine ligand are similar in all proteins.